

9336  
NACA TN 3034



# NATIONAL ADVISORY COMMITTEE FOR AERONAUTICS

TECHNICAL NOTE 3034

GRAPHICAL SOLUTION OF SOME AUTOMATIC-CONTROL PROBLEMS  
INVOLVING SATURATION EFFECTS WITH APPLICATION  
TO YAW DAMPERS FOR AIRCRAFT

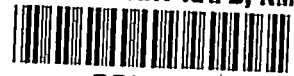
By William H. Phillips

Langley Aeronautical Laboratory  
Langley Field, Va.



Washington  
October 1953

AFM C  
NATIONAL LIBRARY  
AEL 2011



---

TECHNICAL NOTE 3034

---

GRAPHICAL SOLUTION OF SOME AUTOMATIC-CONTROL PROBLEMS  
INVOLVING SATURATION EFFECTS WITH APPLICATION  
TO YAW DAMPERS FOR AIRCRAFT

By William H. Phillips

SUMMARY

A graphical method is presented for determining the motion of a freely oscillating system of one degree of freedom stabilized by a controlling device which applies control force in proportion to the displacement of the system, to its rate of change of displacement, or both. The controlling member is assumed to have limitations on its maximum deflection and on its maximum rate of movement. Several examples are presented to illustrate the method.

From these examples, it is shown that, at sufficiently small amplitudes, the period and damping of the system correspond to those provided by linear operation of the control whereas, at very large amplitudes, the period and damping approach those of the uncontrolled system. At intermediate amplitudes, if the deflection of the control is limited, a smooth transition between these two conditions of period and damping takes place whereas, if the rate of control movement is limited, the damping may be reduced below that of the uncontrolled system. In some cases, limiting the rate of control movement may produce instability over a range of amplitudes.

If the control produces primarily an increase in damping, the control remains effective in producing damping even at amplitudes several times that at which saturation effects are first encountered. This effect may be useful in reducing the power requirements of yaw dampers for airplanes.

INTRODUCTION

Autopilots and other automatic control devices are frequently designed on the basis of linearized theory. In practice, however, the limits of linear operation of these devices may be frequently exceeded.

In some cases, the use of a system designed to exceed its linear range may be advantageous. For example, recent flight tests of devices intended to improve the damping of the lateral oscillations of airplanes have shown that large increases in damping are required only at small amplitudes of oscillation. For this reason, it may be desirable to reduce the power and force output of the controlling device by limiting either its deflection range, its maximum rate of movement, or both, in order that the device may be made as small and as light as possible. In practice, such a control would frequently be required to operate in the range of amplitudes where these limitations are reached. Calculation of the effects of the device under these conditions is therefore of interest.

In electrical work, effects resulting from operating beyond the linear range of a device have been called saturation effects. An analysis of the motion of a control system when saturation effects are involved may frequently be accomplished by conventional methods but the process is tedious, particularly when a number of initial conditions are to be investigated. Problems of this type may be conveniently solved by use of an electric analog computer (refs. 1 and 2) provided such equipment is available. If an analytical solution is required, or if an analytical check on the results obtained from an analog computer is desired, a simple graphical procedure for solving such problems may be of interest.

A method frequently found convenient by previous investigators for analyzing nonlinear systems is the use of the phase plane. This plane, which consists of a plot of the velocity of the system against its displacement, has been used by N. Minorsky (ref. 3) and others for the study of problems involving nonlinear force variations. The same method has been applied by Herbert K. Weiss (refs. 4 and 5) to a study of relay servomechanisms which involve discontinuous force variations. By a slight modification of the usual phase-plane technique, Irmgard Flügge-Lotz (ref. 6) has obtained solutions for the motion of an oscillatory system such as an aircraft controlled by discontinuous or on-off controls. In the present report, methods somewhat similar to those used in reference 6 are applied to the solution of some problems involving saturation effects.

The following analysis is applied to the case of a freely oscillating system with one degree of freedom stabilized by a controlling device which applies control force in proportion to the displacement of the system, to its rate of change of displacement, or both. The controlling member is assumed to have limitations on its maximum deflection and on its maximum rate of movement. Graphical solutions for several problems of this type are presented to illustrate the method.

## SYMBOLS

A, B	constants (see eq. (9))
C	constant, $\sqrt{A^2 + B^2}$
D	differential operator, $d/ds$
$D_c$	differential operator, $d/ds_c$
$I_z$	moment of inertia in yaw
N	yawing moment, or ratio $N_{\delta_r}/N_{\psi}$
R	maximum rate of rudder movement in terms of $s$
r	radius (in polar coordinates)
s	nondimensional measure of time, $\omega_n t$
$\Delta s$	change in nondimensional time
$s_c$	nondimensional measure of time for linear range of operation of control, $s \sqrt{1 + N \frac{\partial \delta_r}{\partial \psi}}$
t	time
x, y	rectangular coordinates (see eqs. (17) and (18))
$\delta_r$	rudder angle
$\theta$	angle (in polar coordinates)
$\Delta \theta$	change in angle $\theta$
$\zeta$	damping ratio of uncontrolled airplane
$\zeta_c$	damping ratio for linear range of operation of control, $\frac{2\zeta + N \frac{\partial \delta_r}{\partial D\psi}}{2 \sqrt{1 + N \frac{\partial \delta_r}{\partial \psi}}}$
$\psi$	angle of yaw

- $\phi$  phase angle,  $\tan^{-1} \frac{A}{B}$
- $\omega$  damped natural frequency of uncontrolled airplane in terms of time unit  $s, \sqrt{1 - \zeta^2}$
- $\omega_c$  damped natural frequency for linear range of operation of control in terms of time unit  $s_c, \sqrt{1 - \zeta_c^2}$
- $\omega_n$  undamped natural frequency of uncontrolled airplane, radians/sec
- $\omega_{nc}$  undamped natural frequency for linear range of operation of control,  $\omega_n \sqrt{1 + N \frac{\partial \delta_r}{\partial \psi}}$ , radians/sec
- $N_\psi = \frac{\partial N}{\partial \psi}$
- $N_{\delta_r} = \frac{\partial N}{\partial \delta_r}$
- $N_{\dot{\psi}} = \frac{\partial N}{\partial \dot{\psi}}$

Subscripts:

- 0 initial value or value at start of an interval
- max maximum value

A dot over quantity denotes differentiation with respect to actual time.

## ANALYSIS

Theoretical development.— An extensive analysis of the motion of missiles under the influence of discontinuous automatic controls is presented in reference 6. This reference employs a modified phase-plane method and contains a detailed development of the theory involved. The theoretical background required for the present analysis is very similar to that utilized in reference 6. In particular, the methods of reference 6 could be employed in the region where the control is

either against its stop or moving at its maximum rate. The methods of reference 6, however, are not convenient for handling the transition from the nonlinear to the linear range of operation. Somewhat different graphical procedures are employed herein to handle this problem. In order to derive these methods, a review of the theory starting with the basic equations of motion appears desirable, although some repetition of the initial development of reference 6 is involved.

In analyses of nonlinear systems by the phase-plane method, the velocity of the system is ordinarily plotted against its displacement. The curve traced out by the system during its motion is called a trajectory in the phase plane. For a single-degree-of-freedom linear system with damping performing a free oscillation, the trajectory may be shown to be a spiral converging on the origin. This spiral is not a true logarithmic spiral but is somewhat distorted. It is shown in reference 6, however, that, if the values of velocity and displacement are plotted on a skewed system of axes, a true logarithmic spiral results. The use of a logarithmic spiral is very advantageous for graphical analysis, inasmuch as all such spirals for a given value of the damping ratio are congruent. As a result, only one spiral for a given value of the damping ratio needs to be plotted. This spiral may then be made to pass through any given point in the plane to fit the desired initial conditions simply by rotation about the origin. In order to obtain the relations required for the graphical construction described herein, expressions are required for the displacement and velocity of the controlled system for various conditions of the control. These expressions are now derived.

For purposes of illustration, the equations of motion are set up for an airplane oscillating in yaw and controlled by the rudder. The same analysis may be applied, however, to any single-degree-of-freedom system obeying similar equations of motion and laws of control. The equation of motion is as follows:

$$I_z \ddot{\psi} - \dot{\psi} N \dot{\psi} - \psi N \dot{\psi} = \delta_r N \delta_r$$

In problems of this type, the number of parameters may be reduced by expressing the oscillatory characteristics in terms of a natural frequency  $\omega_n$  and a damping ratio  $\xi$  which gives the fraction of critical damping (ref. 7). These quantities for the uncontrolled system are defined as follows:

$$\omega_n = \sqrt{-\frac{N_{\dot{\psi}}}{I_z}}$$

$$\xi = -\frac{N_{\dot{\psi}}}{2I_z\omega_n}$$

Also, let  $N = \frac{N_{\delta_r}}{N_{\dot{\psi}}}$ . In terms of these parameters, the equation of motion becomes

$$\ddot{\psi} + 2\xi\omega_n\dot{\psi} + \omega_n^2\psi = -\delta_r N \omega_n^2 \quad (1)$$

A further reduction in the number of parameters may be obtained by use of the nondimensional measure of time  $s = \omega_n t$ . Let

$D = \frac{d}{ds}$ ; equation (1) then becomes

$$D^2\psi + 2\xi D\psi + \psi = -\delta_r N \quad (2)$$

When the system is in its linear range, the rudder angle is proportional either to the angle of yaw, to the yawing velocity, or to a combination of these quantities. The law of control for the rudder in the linear range of operation is therefore

$$\delta_r = \psi \frac{\partial \delta_r}{\partial \psi} + D\psi \frac{\partial \delta_r}{\partial D\psi} \quad (3)$$

When the limits of linear operation are exceeded, the rudder angle is either constant (against a stop) or changing at a constant rate. The rudder angle in this case may be expressed by the equation

$$\delta_r = \delta_{r0} + Rs \quad (4)$$

where  $R$  represents the constant rate of rudder movement in terms of the nondimensional time unit  $s$ . The solutions of the equation of motion for these cases are now discussed.

First, the solution for the linear range of operation is considered. When equation (3) is substituted into equation (2), the following result is obtained:

$$D^2\psi + D\psi \left( 2\xi + N \frac{\partial \delta_r}{\partial D\psi} \right) + \psi \left( 1 + N \frac{\partial \delta_r}{\partial \psi} \right) = 0 \quad (5)$$

Make a second change in the time variable,

$$s_c = s \sqrt{1 + N \frac{\partial \delta_r}{\partial \psi}} \quad (6)$$

and let  $D_c = \frac{d}{ds_c}$ . Equation (5) then changes back to the form of equation (2),

$$D_c^2 \psi + 2\zeta_c D_c \psi + \psi = 0 \quad (7)$$

where

$$\zeta_c = \frac{2\zeta + N \frac{\partial \delta_r}{\partial D\psi}}{2\sqrt{1 + N \frac{\partial \delta_r}{\partial \psi}}} \quad (8)$$

The quantity  $\zeta_c$  represents the damping ratio of the controlled airplane. The natural frequency of the controlled airplane in radians per second is obtained from equations (1), (2), and (5) as

$$\omega_{n_c} = \omega_n \sqrt{1 + N \frac{\partial \delta_r}{\partial \psi}}$$

Before writing down the solution of equation (7), the solution of equation (2) is presented for the case in which the rudder is against a stop or moving at a constant rate. Under these conditions, the right-hand side of the equation is not zero. The solution of equation (7), the right-hand side of which is zero, is then obtained from this result as a special case. When the expression for the rudder angle (eq. (4)) is substituted into equation (2), the solution for the variation of  $\psi$  with  $s$  for specified initial conditions  $\psi_0$ ,  $(D\psi)_0$ , and  $\delta_{r0}$  is as follows:

$$\psi = -N(\delta_{r0} - 2\zeta R) - RNs + e^{-\zeta s}(A \cos \omega s + B \sin \omega s) \quad (9)$$

where

$$\begin{aligned} A &= \psi_0 + N(\delta_{r0} - 2\zeta R) \\ B &= \frac{1}{\omega} \left[ (D\psi)_0 + \zeta \psi_0 + \delta_{r0} N\zeta - (2\zeta^2 - 1)RN \right] \\ \omega &= \sqrt{1 - \zeta^2} \end{aligned}$$



The value of  $D\psi$  may be expressed as a function of  $s$  as follows:

$$D\psi = -RN + e^{-\zeta s}(-\omega A \sin \omega s + \omega B \cos \omega s) - \zeta \left[ \psi + N(\delta_{r0} - 2\zeta R) + RNs \right] \quad (10)$$

The solution of equation (7), which applies when the control is operating in its linear range, may be obtained as a simplified case from expressions (9) and (10), because in this case the form of the differential equation is the same but the right-hand side of the equation is zero. The solution of equation (7) is obtained by setting  $\delta_{r0}$  and  $R$  equal to zero and by substituting  $\zeta_c$  and  $D_c$  for  $\zeta$  and  $D$  in equations (9) and (10).

The derivation of the relations required for the graphical construction, in which the motion is represented by a true logarithmic spiral rather than by a distorted spiral, is now presented. From equations (2) and (4)

$$D^2\psi + 2\zeta D\psi = -\psi - (\delta_{r0} + Rs)N \quad (11)$$

Substituting the value of  $\psi$  from equation (9) into equation (11) yields the relation

$$-D^2\psi - 2\zeta(D\psi + RN) = e^{-\zeta s}(A \cos \omega s + B \sin \omega s) \quad (12)$$

By rearranging equation (10), the following equation is obtained:

$$D\psi + RN + \zeta \left[ \psi + N(\delta_{r0} - 2\zeta R) + RNs \right] = \omega e^{-\zeta s}(-A \sin \omega s + B \cos \omega s) \quad (13)$$

In equations (12) and (13), set

$$A = C \sin \phi$$

$$B = C \cos \phi$$

where  $C = \sqrt{A^2 + B^2}$  and  $\phi = \tan^{-1} \frac{A}{B}$ . Equation (12) then becomes

$$\begin{aligned} \omega \left[ -D^2\psi - 2\zeta(D\psi + RN) \right] &= \omega C e^{-\zeta s} (\sin \phi \cos \omega s + \cos \phi \sin \omega s) \\ &= \omega C e^{-\zeta s} \sin (\omega s + \phi) \end{aligned} \quad (14)$$

Equation (13) becomes

$$\begin{aligned} D\psi + RN + \zeta \left[ \psi + N(\delta_{r_0} - 2\zeta R) + RNs \right] &= \omega C e^{-\zeta s} (\sin \phi \sin \omega s + \cos \phi \cos \omega s) \\ &= \omega C e^{-\zeta s} \cos (\omega s + \phi) \end{aligned} \quad (15)$$

The values on the right-hand sides of equations (14) and (15) may be identified as the rectangular coordinates of a logarithmic spiral which, in polar coordinates, has the formula

$$r = r_0 e^{-\zeta \theta / \omega} \quad (16)$$

where  $\theta = \omega s + \phi$  and  $r_0 = \omega C e^{\zeta \phi / \omega}$ .

In a set of rectangular coordinates, therefore, values of  $x$  and  $y$  are plotted such that

$$x = \omega \left[ -D^2\psi - 2\zeta(D\psi + RN) \right] \quad (17)$$

$$y = D\psi + RN + \zeta \left[ \psi + N(\delta_{r_0} - 2\zeta R) + RNs \right] \quad (18)$$

The resulting curve, which represents a trajectory of the motion, is a logarithmic spiral centered at the origin. In practice, the initial angle  $\phi$ , which is related to the initial conditions of the problem, never has to be determined because, as mentioned previously, a logarithmic spiral may be rotated about the origin to pass through any point without changing its shape. A relationship given with equation (16) shows that the nondimensional time elapsing for any change in the angular coordinate  $\theta$  is given by

$$\Delta s = \frac{\Delta \theta}{\omega}$$

The convergence of the spiral is determined by the exponential factor  $\zeta/\omega$ . (Actually, only one variable is involved because, as stated in connection with eq. (9),  $\omega = \sqrt{1 - \zeta^2}$ .)

The coordinate system for the logarithmic spiral, of course, differs from the velocity-displacement coordinate system ordinarily used in phase-plane studies. From the rectangular coordinates  $x$  and  $y$ , however, the values of  $D^2\psi$ ,  $D\psi$ , and  $\psi$  may be determined as follows: First, eliminate  $\psi$  between equations (11) and (18). The result is

$$y = D\psi(1 - 2\zeta^2) - \zeta D^2\psi + RN(1 - 2\zeta^2) \quad (19)$$

Equations (17) and (19) express  $x$  and  $y$  in terms of  $D\psi$  and  $D^2\psi$ . If the value of  $D\psi$  is eliminated between equations (17) and (19),

$$y = -\frac{D^2\psi}{2\xi} - \frac{(1 - 2\xi^2)x}{2\xi\omega} \quad (20)$$

Equation (20) allows lines of constant yawing acceleration  $D^2\psi$  to be drawn in the  $x,y$  plane. These lines are straight lines with a slope  $-\frac{1 - 2\xi^2}{2\xi\omega}$ . The line for  $D^2\psi = 0$  passes through the origin.

If the value of  $D^2\psi$  is eliminated between equations (17) and (19),

$$y = D\psi + RN + \frac{\xi x}{\omega} \quad (21)$$

Equation (21) allows lines of constant yawing velocity  $D\psi$  to be drawn in the  $x,y$  plane. These lines are straight lines with the slope  $\xi/\omega$ . The line for  $D\psi = -RN$  passes through the origin.

In order to determine the angle of yaw  $\psi$ , substitute  $D^2\psi + 2\xi D\psi$  from equation (11) into equation (17). The result is an alternate definition of  $x$ ,

$$x = \omega \left[ \psi + N(\delta_{r0} - 2\xi R) + RNs \right] \quad (22)$$

This equation shows that lines of constant  $\psi$  are parallel to the  $y$ -axis. The grid of lines of constant  $\psi$  is moving across the  $x,y$  plane at a constant rate for the case in which the rudder is moving at a constant rate. This result is shown by the term  $RNs$ , which represents a shift in the origin of the grid of  $\psi$  lines by an amount proportional to the nondimensional time  $s$ .

Because such a moving grid is inconvenient for graphical work, the value of  $\psi$  may be obtained more easily for the case in which the rudder is moving at a constant rate by reading values of  $D\psi$  and  $D^2\psi$  from their fixed grids and using equation (11) to determine the value of  $\psi$ . For the case where the rudder angle is constant, however, the value of  $R$  is zero, and equation (22) reduces to

$$x = \omega \left( \psi + N\delta_{r0} \right) \quad (23)$$

In this case, lines of constant  $\psi$  are fixed lines, parallel to the  $y$ -axis. The line for  $\psi = -N\delta_{r0}$  passes through the origin.

The geometrical relationship among the three sets of grid lines for reading  $D^2\psi$ ,  $D\psi$ , and  $\psi$  is shown in figure 1. This relationship may be derived from equations (20), (21), and (23). The grid lines for  $D\psi$  constant are rotated from the horizontal by the angle  $\tan^{-1} \frac{\xi}{\omega}$ ; the grid lines for  $D^2\psi$  constant are rotated from the vertical by twice this angle, which equals  $\tan^{-1} \frac{2\xi\omega}{1 - 2\xi^2}$ . The spacing between grid lines for  $D^2\psi = 0$  and  $D^2\psi = 1$  is shown to be one unit when measured along a line of constant  $D\psi$ . Similarly, the spacing between the lines for  $D\psi = 0$  and  $D\psi = 1$  is one unit when measured along a line of constant  $D^2\psi$ . The spacing of the grid lines for reading  $\psi$  is such that these grid lines would pass through the intersections of a grid line for  $D\psi$  constant and the various grid lines for  $D^2\psi$ . These geometric relationships may be useful in constructing the grids for graphical work. The grids drawn in figure 1 are shown centered at the origin of the  $x$  and  $y$  coordinates, which is the origin of the spiral. In use, however, the line  $D\psi = 0$  often does not pass through the origin of the spiral because, as shown by equation (21), the line for  $D\psi = -R\dot{N}$  passes through the origin when the rudder is moving at a constant rate. The spacing and direction of the grid lines, however, are the same as those shown in figure 1. Similarly, the grid for reading  $\psi$  is often moved laterally with respect to the other grids while its direction is maintained parallel to the  $y$ -axis.

Application of theory.- The results just presented are now summarized briefly and an attempt is made to show their physical meaning. The analysis considers the motion of a linear system of one degree of freedom under the influence of a linearly increasing force (corresponding to a constant rate of rudder deflection), a constant force (corresponding to a fixed rudder deflection), or zero force (corresponding to motion in the linear range of operation). In each case, the motion is represented by a logarithmic spiral in a certain system of coordinates designated the  $x,y$  plane. Values of  $D^2\psi$ ,  $D\psi$ , and  $\psi$  may be read from suitable grids of lines superimposed on this plane.

In the case of a linearly increasing force, the displacement of a single-degree-of-freedom system is known to increase linearly with time after the transient oscillation has damped. The velocity of the system approaches a constant value, and the acceleration approaches zero. This behavior agrees with that given by equations (22), (21), and (20), which show that the grid of lines of angle of yaw move across the  $x,y$  plane at a constant rate, whereas the spiral representing the motion converges to a certain value of yawing velocity and to a value of yawing acceleration of zero.

The simpler cases of a constant force or of zero force may be shown to correspond to equations (22), (21), and (20) in a similar manner. In the case of a constant force, the displacement approaches a constant value, and the velocity and acceleration both approach zero. In the case of zero force, all three quantities approach zero. The origins of the grids for reading  $D^2\psi$ ,  $D\psi$ , and  $\psi$  for this condition all coincide with the origin of the spiral. The tilt of the grid lines for reading values of  $D\psi$  and  $D^2\psi$  results from the fact that, when a single-degree-of-freedom system with damping performs a free oscillation, the velocity leads the displacement by  $90^\circ$  plus the angle  $\tan^{-1} \frac{\zeta}{\omega}$  and the acceleration leads the velocity by  $90^\circ$  plus the same angle. These relationships were pointed out by R. K. Mueller in reference 8. The present analysis shows that this same concept can be extended to the case of the system under the influence of a constant force or a linearly increasing force, but that a special coordinate system is required to take into account the constant and linearly increasing terms in the solution for the transient motion as well as the term representing the damped oscillation.

In order to make a graphical solution of the motion of the system for specified values of the variables, suitable spirals and grids should be constructed. One spiral is required for the linear range of operation, based on the damping ratio  $\zeta_c$  of the controlled system. Another spiral is required for the saturated range of operation, based on the damping ratio  $\zeta$  of the uncontrolled system. A suitable set of grids for each of the spirals should be prepared on separate sheets of tracing paper. These grids may then be superimposed on the spirals with the origins located to represent the various conditions of constant rudder rate, constant rudder deflection, or linear operation of the control. The procedure for obtaining a solution consists in tracing the trajectory representing the motion of the system, with suitable shifts in the grids or changes in the spiral at points where the mode of operation changes from one regime to another. (These points are called "switch points" in ref. 6.) The correct procedure for making these shifts is best described by means of specific examples. Several such examples are now presented.

#### EXAMPLES

Five examples are presented to illustrate different features of the method. These examples are summarized in the following table:

Example	Control type: Rudder angle proportional to -	Limitation
I	Yawing velocity	Rudder rate limited
II	Yawing velocity	Rudder deflection limited
III	Angle of yaw	Rudder rate limited
IV	Angle of yaw	Rudder deflection limited
V	Angle of yaw and yawing velocity	Both rudder rate and deflection limited

Specific values for the parameters and initial conditions are assumed for each example. No attempt is made to investigate a range of these parameters or initial conditions.

Example I. - The following parameters are assumed:

$$\frac{\partial \delta_r}{\partial D\psi} = 1$$

$$\zeta = 0.05 \quad (\omega = 0.9987)$$

$$N = 0.3$$

$$R = \pm 0.125$$

from which may be derived, from equation (8),

$$\zeta_c = 0.2 \quad (\omega_c = 0.9798)$$

The following initial conditions are assumed:

$$\psi_0 = -0.531$$

$$(D\psi)_0 = 0$$

$$\delta_{r0} = -0.25$$

from which may be derived, from equation (11),

$$(D^2\psi)_0 = 0.606$$

Two spirals should be constructed, corresponding to values of damping

ratio of 0.05 and 0.2. A typical spiral, with the associated grids for reading  $D^2\psi$  and  $D\psi$ , is shown in figure 2. A convenient and sufficiently accurate method of constructing a logarithmic spiral as a succession of circular arcs is presented in reference 6 (pt. 1, appendix I, p. 41).

In figure 2, the x- and y-scales are drawn on the same graph as the spiral. This representation is correct, inasmuch as the x- and y-scales are in all cases considered to be centered at the origin of the spiral. When the spiral is used, however, it must ordinarily be rotated about its origin to pass through the desired initial point. If the spiral is rotated, the x- and y-scales do not rotate but remain fixed in direction. In practice, therefore, the values of x and y are read with a ruler rather than from scales marked on the same sheet as the spiral.

The graphical work for example I is shown in figure 3. In this figure and succeeding figures in which graphical solutions are shown, the scales labeled x and y are drawn, for convenience, with their origin at the origin of the grid for  $D^2\psi$  and  $D\psi$ . These scales should be considered to show only the direction and spacing but not the true position of the x- and y-scales, because the x- and y-scales are in all cases considered to be centered at the origin of the spiral, which is shifted in various parts of the solution. These scales therefore move when the origin of the spiral changes.

In the linear range of operation,  $\delta_r = D\psi \frac{\partial \delta_r}{\partial D\psi}$ . The quantity  $D\psi \frac{\partial \delta_r}{\partial D\psi}$  (called the "control function" in ref. 6) determines the rudder position called for by the controlling mechanism. Since initially the control function  $D\psi \frac{\partial \delta_r}{\partial D\psi} = 0(1) = 0$  whereas  $\delta_{r0} = -0.25$ , the rudder is not in the position called for by the controlling mechanism and will run at its maximum rate in the direction to reduce the error between its existing position and the position called for by the controlling mechanism. These conditions establish that the initial interval of the motion takes place with the rudder moving at a constant rate in the positive direction. The spiral corresponding to  $\xi = 0.05$  should therefore be used. From formulas (20) and (21), the origin of the spiral should be located at the intersection of the grid lines  $D^2\psi = 0$  and  $D\psi = -RN = -(0.125)(0.3) = -0.0375$ . The spiral may now be rotated so that it passes through the initial point  $(D\psi)_0 = 0$ ,  $(D^2\psi)_0 = 0.606$ . The section of the spiral corresponding to the first interval may then be traced in as shown in figure 3(a). The ends of the intervals, which correspond to changes in the direction of motion of the rudder or to changes in the mode of operation, are shown in figure 3 by circled

points which are numbered to correspond to the number of the interval. The radial line from the origin of the spiral passing through the initial point corresponds to  $s = 0$ . Values of  $D^2\psi$  and  $D\psi$  may be read from the grids at successive values of the radial angle  $\theta$  measured from this radial line. For each value of  $\theta$ , the corresponding value of nondimensional time is determined from the formula  $s = \frac{\theta}{\omega}$ . If desired, the values of  $\psi$  may be determined at the same points by substituting the values of  $D^2\psi$ ,  $D\psi$ , and  $s$  into equation (11).

As the motion continues, the error between the rudder angle existing and that called for by the control is eventually reduced to zero. At this point the interval ends. This condition exists when

$$\delta_r = \delta_{r0} + R s = D\psi \frac{\partial \delta_r}{\partial D\psi}$$

Make the substitution  $s = \frac{\theta}{\omega}$  and solve for  $D\psi$ . Then,

$$D\psi = \frac{\delta_{r0} + R \frac{\theta}{\omega}}{\frac{\partial \delta_r}{\partial D\psi}}$$

The curve showing  $D\psi$  as a function of  $\theta$  satisfying this relation is shown in figure 3 as a short dashed line. The intersection of this curve and the spiral determines the time at which the rudder reaches the angle called for by the control. Substitution of a few values of  $\theta$  into this equation will quickly show the values of  $\theta$  that will give values of  $D\psi$  close to those required to intersect the spiral. As a result, only two or three points of the curve in the vicinity of the intersection need to be plotted.

An alternate method for determining the time at which the rudder reaches the angle called for by the control is to carry along an auxiliary plot of the rudder angle  $\delta_r$  and the control function  $D\psi \frac{\partial \delta_r}{\partial D\psi}$  as functions of  $s$ . The intersection of these curves then determines the desired time. This type of plot is also valuable in giving a physical picture of the action of the control.

When the rudder reaches the angle called for by the control, a check must be made to find whether the system will thereafter operate linearly or whether the maximum rate called for will again exceed that available. The rate of rudder motion called for by the control is

$$D\delta_r = D^2\psi \frac{\partial \delta_r}{\partial D\psi}$$



Because the maximum rate available is  $R$ , this condition can be satisfied only when

$$D^2\psi = \frac{R}{\partial\delta_r/\partial D\psi}$$

A pair of grid lines determined by this relation  $\left(D^2\psi = \pm \frac{0.125}{1}\right)$  is shown in figure 3. The area between these lines is designated as the "linear band." Whenever the rudder reaches the angle called for by the control at a point within the area bounded by these two lines, the control operates linearly, and the graphical analysis must be continued with the spiral for  $\xi_c = 0.2$ . Whenever the trajectory passes outside the area bounded by these two lines, however, the rudder is moving at its maximum rate and the analysis must be made by using the spiral for  $\xi = 0.05$ . Note that the trajectory may pass through the linear band without the control operating linearly. Only when the rudder reaches the angle called for by the control within the linear band does the control operate linearly.

The trajectory for the first interval of the motion is seen from figure 3(a) to end outside the band of linear operation. The rudder therefore reverses and moves at its maximum rate in the negative direction for the next interval. The spiral is therefore shifted so that its origin is located at the intersection of the grid lines  $D^2\psi = 0$  and  $D\psi = -RV = -(-0.125)(0.3) = 0.0375$ . The spiral is then rotated to pass through the final point of the first interval, which becomes the initial point of the second interval. Values of  $\theta$  and  $s$  for this interval, starting from zero at the start of the interval, must be determined. These values of  $\theta$  and  $s$  are used in determining the values of  $\psi$  for this interval and the end point of the interval. Finally, the values of  $s$  in the second interval are added to those in the first interval to determine the over-all time elapsed. The end of the second interval is determined in the same way as the end of the first interval.

The analysis is continued in this manner for several intervals, the origin of the spiral being shifted each time the rudder motion reverses. As shown in figure 3(a), the end point of the fifth interval occurs within the band of linear operation. At this point, the work must be continued on the spiral for  $\xi_c = 0.2$ . In transferring the work to the spiral for the linear mode of operation, allowance must, in general, be made for the fact that this spiral is based on equation (7), which is expressed in terms of the time unit  $s_c$  (eq. (6)). For this reason, the derivatives  $D^2\psi$  and  $D\psi$  and the limits of the linear band must be converted to the new time unit whenever the work is continued on the spiral for the linear range. The required relations are

$$D_c^2\psi = \frac{D^2\psi}{1 + N \frac{\partial \delta_r}{\partial \psi}}$$

$$D_c\psi = \frac{D\psi}{\sqrt{1 + N \frac{\partial \delta_r}{\partial \psi}}}$$

Time as measured on this spiral must be converted back to units of  $s$  when plotting the results. In the present example,  $s = s_c$ ,  $D_c^2\psi = D^2\psi$ , and  $D_c\psi = D\psi$  because  $\partial \delta_r / \partial \psi$  is zero. The transformation therefore has no effect in this case.

The spiral for  $\zeta_c = 0.2$  is located on its own grids so that its origin is at  $D^2\psi = 0$ ,  $D\psi = 0$ . Values of  $D^2\psi$  and  $D\psi$  from the last point are replotted on these grids and the spiral is rotated to pass through this point, as shown in figure 3(b). The work then proceeds as before.

In the example chosen, the motion almost immediately passes outside of the band of linear operation again. The analysis is therefore shifted back to the spiral for  $\zeta = 0.05$  for the seventh interval. This interval again ends in the linear range, and thereafter the motion remains linear and damps out exponentially.

Time histories of the yaw angle  $\psi$ , the control function  $D\psi \frac{\partial \delta_r}{\partial D\psi}$ , and the rudder angle  $\delta_r$ , obtained from the preceding analysis, are plotted in figure 4.

Example II.— The following parameters are assumed:

$$\frac{\partial \delta_r}{\partial D\psi} = 1$$

$$\zeta = 0.05 \quad (\omega = 0.9987)$$

$$N = 0.3$$

$$\delta_{r_{\max}} = \pm 0.125$$

from which may be derived, from equation (8),

$$\zeta_c = 0.2 \quad (\omega_c = 0.9798)$$

The following initial conditions are assumed:

$$\psi_0 = -0.575$$

$$(D\psi)_0 = 0$$

Since the rudder is constrained to move in proportion to the yawing velocity as long as it is not against a stop,

$$\delta_{r0} = 0$$

From equation (11) the following equation may be derived:

$$(D^2\psi)_0 = 0.575$$

The graphical work for this problem is shown in figure 5. This example illustrates a procedure not found in example I in that the angle of yaw may be read from suitable sets of vertical grid lines whenever the rudder is against a stop. These grid lines cannot be used when the rudder is moving at a constant rate. Initially, the control is operating in its linear range; therefore, the spiral for  $\xi_c = 0.2$  is used for the first interval (fig. 5(a)), with its origin located at  $D^2\psi = 0$ ,  $D\psi = 0$ . The rudder always reaches its stop at a given value of yawing velocity, because  $\delta_r = D\psi \frac{\partial \delta_r}{\partial D\psi}$ . The values of  $D\psi$  where the rudder reaches its stops are

$$D\psi = \pm \frac{\delta_{r\max}}{\partial \delta_r / \partial D\psi} = \pm \frac{0.125}{1} = \pm 0.125$$

These lines are shown as limits of the linear band in figure 5. When the trajectory passes outside one of these lines, the work must be continued on the spiral corresponding to  $\xi = 0.05$ . This spiral is centered on the grid lines  $D^2\psi = 0$ ,  $D\psi = 0$ , as shown by equations (20) and (21). Values of  $s$  may be determined at each point on the trajectory as described for example I. If desired, values of  $\psi$  may be obtained from the values of  $D^2\psi$  and  $D\psi$ , as described for example I, or they may be read directly from suitable sets of vertical grid lines constructed in accordance with equation (23). This equation shows that the line for  $\psi = -N\delta_{r0}$  passes through the origin of the spiral. When the trajectory is above the line  $D\psi = 0.125$ , therefore, the grid line  $\psi = -(0.3)(0.125) = -0.0375$  passes through the origin. When the trajectory is below the line  $D\psi = -0.125$ , the grid line  $\psi = 0.0375$  passes through the origin. When the system is operating in the linear

range, of course, the grid line  $\psi = 0$  passes through the origin. The grid lines corresponding to these conditions are shown by dotted lines in figure 5.

Time histories of the yaw angle  $\psi$ , the control function  $D\psi \frac{\partial \delta_r}{\partial D\psi}$ , and the rudder angle  $\delta_r$  obtained for this problem are plotted in figure 6.

Example III.- The following parameters are assumed:

$$\frac{\partial \delta_r}{\partial \psi} = 2$$

$$\zeta = 0.05 \quad (\omega = 0.9987)$$

$$N = 0.3$$

$$R = \pm 0.125$$

from which may be derived, from equation (8),

$$\zeta_c = 0.0395 \quad (\omega_c = 0.9992)$$

The following initial conditions are assumed:

$$\psi_0 = -0.5$$

$$(D\psi)_0 = 0$$

$$\delta_{r0} = -0.25$$

from which may be derived, from equation (11),

$$(D^2\psi)_0 = 0.575$$

The graphical work for this problem is shown in figure 7, curve 1. The procedure required is very similar to that of example I, although different equations are required to determine the end points of the intervals and the limits of the linear band.

The end of an interval is reached when

$$\delta_r = \delta_{r0} + R\psi = \psi \frac{\partial \delta_r}{\partial \psi} \quad (24)$$

From equation (22), the value of  $\psi$  may be obtained as follows:

$$\psi = \frac{x}{\omega} - N(\delta_{r0} - 2\zeta R) - RNs \quad (25)$$

Substitute equation (25) into equation (24), replace  $s$  by  $\theta/\omega$ , and solve for  $x$ . The result is

$$x = \theta R \left( N + \frac{1}{\partial \delta_r / \partial \psi} \right) + \delta_{r0} \omega \left( N + \frac{1}{\partial \delta_r / \partial \psi} \right) - 2\zeta \omega R N \quad (26)$$

Numerical values may be substituted into equation (26) to obtain  $x$  as a function of  $\theta$ . A curve of  $x$  as a function of  $\theta$  satisfying this relation may be plotted on the graph, as shown in figure 7 by a dashed line. The intersection of this curve and the spiral determines the time at which the rudder reaches the angle called for by the control. When the values of  $x$  and  $\theta$  are plotted, it must be remembered that the  $x$ - and  $y$ -axes are considered to pass through the origin of the spiral, not the origin of the  $D^2\psi$ ,  $D\psi$  grid as shown in the figures. Furthermore, values of  $\theta$  are measured about the origin of the spiral.

The complete solution may now be carried out as it was in the previous examples. This solution, shown in figure 7, curve 1, indicates that the motion approaches a steady hunting oscillation at an amplitude slightly smaller than the initial amplitude. Time histories of the

control function  $\psi \frac{\partial \delta_r}{\partial \psi}$  and the rudder angle  $\delta_r$ , obtained from the preceding analysis, are plotted in figure 8(a).

In order to show the behavior of the system when the motion is started with smaller initial amplitudes, curves 2, 3, and 4 of figure 7 were plotted. The resultant time histories are shown in figures 8(b) to 8(d). These results indicate that, if the motion exceeds the linear range only slightly, as in curve 3, the oscillation continues to build up until the steady hunting condition of curve 1 is approached. On the other hand, if the oscillation starts at a slightly smaller amplitude, as in curve 4, it remains stable and damps out. Note that in the solution for the linear range of operation (fig. 7(b)) a transformation of the time scale is required.

Example IV.— The following parameters are assumed:

$$\frac{\partial \delta_r}{\partial \psi} = 2$$

$$\zeta = 0.05 \quad (\omega = 0.9987)$$

$$N = 0.3$$

$$\delta_{r_{\max}} = \pm 0.250$$

from which may be derived, from equation (8),

$$\zeta_c = 0.0395 \quad (\omega_c = 0.9992)$$

The following initial conditions are assumed:

$$\psi_0 = -0.575$$

$$(D\psi)_0 = 0$$

The control attempts to move the rudder in accordance with the relation  $\delta_r = \psi \frac{\partial \delta_r}{\partial \psi}$ . Initially, the control calls for a value of  $\delta_r$  equal to  $(-0.575)(2) = -1.15$ , which is greater than the maximum rudder deflection. The initial rudder angle is therefore the maximum value.

$$\delta_{r0} = -0.25$$

From equation (11) the following equation may be derived:

$$(D^2\psi)_0 = 0.650$$

The graphical work for this problem is shown in figure 9. Time histories of the control function  $\psi \frac{\partial \delta_r}{\partial \psi}$  and the rudder angle  $\delta_r$  are plotted in figure 10.

Example V.— The following parameters are assumed:

$$\frac{\partial \delta_r}{\partial \psi} = 2$$

$$\frac{\partial \delta_r}{\partial D\psi} = 1$$

$$\zeta = 0.05 \quad (\omega = 0.9987)$$

$$N = 0.3$$

$$R = \pm 0.2$$

$$\delta_{r_{\max}} = \pm 0.25$$

from which may be derived, from equation (8),

$$\zeta_c = 0.158 \quad (\omega_c = 0.9874)$$

The following initial conditions are assumed:

$$\psi_0 = -0.325$$

$$(D\psi)_0 = 0$$

$$\delta_{r0} = -0.25$$

from which may be derived, from equation (11),

$$(D^2\psi)_0 = 0.4$$

In this problem, the graphical work for which is shown in figure 11, curve 1, somewhat more complicated relations exist for determining

the limits of linear operation. The quantity  $\psi \frac{\partial \delta_r}{\partial \psi} + D\psi \frac{\partial \delta_r}{\partial D\psi}$  determines the rudder position called for by the controlling mechanism. Initially, this quantity equals -0.650, whereas the rudder is against its negative stop at -0.25. The rudder therefore stays at its negative stop for the first interval. The rudder leaves its stop when the control function

$$\psi \frac{\partial \delta_r}{\partial \psi} + D\psi \frac{\partial \delta_r}{\partial D\psi} = -0.25$$

This relation determines a straight line on the  $\psi$  and  $D\psi$  grids which may be drawn in as shown in figure 11. A similar line is drawn to show when the rudder leaves its positive stop.

After the rudder leaves its stop, a check must be made to determine whether the rudder will operate in the linear range. The rate of rudder motion called for by the control is

$$D\delta_r = D\psi \frac{\partial \delta_r}{\partial \psi} + D^2\psi \frac{\partial \delta_r}{\partial D\psi}$$

A second pair of lines determined by this relation,  $\pm 0.2 = D\psi(2) + D^2\psi(1)$ , is shown in figure 11. The area bounded by the two pairs of lines is designated as the "linear region" in the figure. Since the first interval ends outside the area bounded by these lines, the rudder moves at its maximum rate in the positive direction for the second interval. The solution proceeds as in case I or III.

The second interval ends when the rudder reaches its maximum deflection or when it reaches the angle called for by the control, whichever occurs first. The time that the rudder must travel to reach its positive stop after the start of an interval is determined from the relation

$$\delta_{r0} + R s = \delta_{r_{\max}}$$

from which

$$s = \frac{\theta}{\omega} = \frac{-\delta_{r0} + \delta_{r_{\max}}}{R}$$

The value of  $\theta$  at which this condition is satisfied, in the present instance, is

$$\theta = (0.9987) \frac{-(-0.25) + 0.25}{0.2} = 2.49 \text{ radians} = 143^\circ$$

The conditions under which the rudder reaches the angle called for by the control are given by the formula

$$x \left[ -\omega \frac{\partial \delta_r / \partial D\psi}{\partial \delta_r / \partial \psi} \tan(\theta_0 + \theta) - \frac{\partial \delta_r / \partial D\psi}{\partial \delta_r / \partial \psi} + 1 \right] = \theta R \left( N + \frac{1}{\partial \delta_r / \partial \psi} \right) + \delta_{r0} \omega \left( N + \frac{1}{\partial \delta_r / \partial \psi} \right) - RN\omega \left( 2\xi - \frac{\partial \delta_r / \partial D\psi}{\partial \delta_r / \partial \psi} \right)$$

In this formula,  $\theta_0$  is the angle between the positive x-axis and the initial point of the interval, measured clockwise. This equation is an extension of equation (26) to the present problem and is derived in a similar manner. A few points of a curve of  $x$  as a function of  $\theta$  satisfying this relation may be plotted on the graph. The intersection of this curve and the spiral determines the time at which the rudder reaches the angle called for by the control. Alternatively, a plot of the rudder angle and the control function as functions of  $s$  may be made to determine this point.

In the present instance, the rudder reaches its positive stop before it reaches the angle called for by the control. In the third interval, therefore, the rudder is against its positive stop. The solution proceeds as it did for the first interval.

Continuation of the solution, shown in figure 11, curve 1, results in a closed cycle. The system therefore performs a steady hunting oscillation for the initial conditions chosen. Time histories of the

yaw angle  $\psi$ , the control function  $\psi \frac{\partial \delta_r}{\partial \psi} + D\psi \frac{\partial \delta_r}{\partial D\psi}$ , and the rudder angle  $\delta_r$  obtained from the preceding analysis are plotted in figure 12(a).



In order to show the behavior of the system when the motion is started with a smaller initial amplitude, curve 2 of figure 11 was plotted. This solution differs from that of curve 1 in that at the end of the first interval the rudder reaches the angle called for by the control before it reaches its positive stop. The details of the graphical work are somewhat similar to those required for example I. Time histories of the motion are shown in figure 12(b).

## DISCUSSION OF RESULTS

Although the preceding discussion is intended primarily to describe a graphical method for determining the motion of an automatically controlled system when saturation effects are present, a few results of interest may be obtained from the examples presented.

Variation of stability with amplitude.- First, some general statements may be made regarding the variation of the stability of a system of the type considered as a function of amplitude. At amplitudes within the linear range of operation of the control, the period and damping may be predicted by well-known methods. For practical controls, of course, the damping should usually be considerably greater than that of the uncontrolled system. At very large amplitudes, far beyond those where the linear range is first exceeded, the period and damping of the system approach those of the uncontrolled system. This tendency results from the fact that the moments supplied by the control, when either its deflection or rate is limited, are very small compared with the inherent restoring and damping moments acting on the system at sufficiently large amplitudes. At intermediate amplitudes, the behavior of the system depends on how the saturation effects influence the phase relationship between the motion of the system and that of the control. If only the control deflection is limited, as in example II or IV, the phase relationship tends to be unaffected, and a smooth transition occurs between the characteristics of the controlled system and that of the uncontrolled system as the amplitude is increased. If only the control rate is limited, however, as in example I or III, a phase lag approaching  $90^\circ$  in the motion of the control is introduced and, as a result, the damping at intermediate amplitudes is decreased. Whether actual instability occurs in some amplitude range depends primarily on the amount of damping present in the uncontrolled system and in the controlled system in its linear range of operation. In example III presented previously (fig. 8), instability occurred at an amplitude slightly beyond the linear range and continued up to several times this amplitude. With both rate and deflection limited, a phase lag intermediate between those produced by the rate and deflection limitations may be present. If the deflection range is sufficiently

large, however, the rate limitation may prevent the control from ever reaching its stops; therefore the deflection limitation becomes unimportant.

Examples I and II, presented previously, in which the control produced primarily an increase in damping, show that the control remained effective in producing damping even at amplitudes several times that at which the saturation effects were first encountered (figs. 4 and 6). This result may be of importance in the design of yaw dampers for airplanes because it indicates that, if some decrease in damping at the larger amplitudes can be tolerated, the power output of the controlling device may be made considerably less than that required to provide linear operation throughout the range of amplitudes encountered. As was previously mentioned, flight tests have shown that increased damping of the lateral oscillations of airplanes is required mainly at small amplitudes.

Extension of the examples to other conditions.- Some reduction in the number of parameters in the problem has already been made by expressing time in terms of the nondimensional parameter  $s$ . The results of any given problem may therefore be applied to systems with any natural frequency by converting back from the nondimensional to the real time unit. A further reduction in the number of parameters is possible by dividing through the equations for the variations of  $\psi$  and  $D\psi$  (eqs. (9) and (10)) by the quantity  $RN$ . The problem is then completely specified in terms of the quantities  $\zeta$ ,  $\delta_r/R$ ,  $\psi/RN$ ,  $D\psi/RN$ ,  $N \frac{\partial \delta_r}{\partial \psi}$ , and  $N \frac{\partial \delta_r}{\partial D\psi}$ . A given solution may therefore be applied to systems with other values of  $R$  and  $N$  provided the initial conditions are changed so that the quantities  $\delta_{r0}/R$ ,  $\psi_0/RN$ , and  $D\psi_0/RN$  remain the same and provided the gearing constants are changed so that the quantities  $N \frac{\partial \delta_r}{\partial \psi}$  and  $N \frac{\partial \delta_r}{\partial D\psi}$  remain the same. Values of  $\delta_r/R$ ,  $\psi/RN$ , and  $D\psi/RN$  obtained from the given solution apply to the new system. The values of  $\delta_r$ ,  $\psi$ , and  $D\psi$  may then be obtained by multiplying these parameters by the appropriate factors.

Application to actual automatic controls.- Although actual automatic controls do not follow the controlling quantities with zero lag as assumed in the foregoing analysis, a method is suggested whereby the same type of analysis may be applied to give approximate solutions for saturation effects on actual automatic controls. For this purpose, the gearing constants  $\partial \delta_r / \partial \psi$  and  $\partial \delta_r / \partial D\psi$  should be selected to give the same amplitude ratio and phase angle between the control motion and the motion of the system as exists on the actual automatic control at the frequency at which the controlled system oscillates in its linear range. Usually this frequency may be approximately determined from elementary considerations. The applicability of this method depends on the condition that the saturation effects do not change the frequency

very much. This condition may be expected to exist when the restoring moment on the uncontrolled system is fairly large compared with the restoring moment supplied by the control. The accuracy of the results obtained by this method probably depends to some extent on the actual details of the mechanism under consideration. This method is limited in applicability to cases in which the controlled member can be approximated as a single-degree-of-freedom system. No limitation is placed on the complexity of the controlling mechanism itself, inasmuch as experimentally determined frequency-response data could be used to select the gearing constants.

### CONCLUSIONS

A graphical method is presented for determining the motion of a freely oscillating system of one degree of freedom stabilized by a controlling device which applies control force in proportion to the displacement of the system, to its rate of change of displacement, or both. The controlling member is assumed to have limitations on its maximum deflection, on its maximum rate of movement, or both. Although the report is intended primarily to describe this graphical method, the following conclusions may be obtained from the examples presented:

1. At sufficiently small amplitudes the period and damping of the system correspond to those provided by linear operation of the control whereas, at very large amplitudes, the period and damping approach those of the uncontrolled system. At intermediate amplitudes, if the deflection of the control is limited, a smooth transition between these two conditions of period and damping takes place whereas, if the rate of control movement is limited, the damping may be reduced below that of the uncontrolled system. In some cases, limiting the rate of control movement may produce instability over a range of amplitudes.

2. If the control produces primarily an increase in damping, the control remains effective in producing damping even at amplitudes several times that at which saturation effects are first encountered. This effect may be useful in reducing the power requirements of yaw dampers for airplanes.

Langley Aeronautical Laboratory,  
National Advisory Committee for Aeronautics,  
Langley Field, Va., August 18, 1953.

## REFERENCES

1. Philbrick, George A.: Discussion of "A Frequency Response Method for Analyzing and Synthesizing Contactor Servomechanisms" by Ralph J. Kochenburger. Trans. Am. Inst. Elec. Eng., vol. 69, pt. I, 1950, p. 283.
2. Edwards, Charles M., and Johnson, E. Calvin, Jr.: An Electronic Simulator for Nonlinear Servomechanisms. Trans. Am. Inst. Elec. Eng., vol. 69, pt. I, 1950, pp. 300-306.
3. Minorsky, N.: Introduction to Non-Linear Mechanics. Edwards Brothers, Inc., 1947.
4. Weiss, Herbert K.: Analysis of Relay Servomechanisms. Jour. Aero. Sci., vol. 13, no. 7, July 1946, pp. 364-376.
5. Weiss, Herbert K.: Analysis of a Friction Damper for Clutch-Type Servomechanisms. Jour. Aero. Sci., vol. 18, no. 10, Oct. 1951, pp. 676-682.
6. Flügge-Lotz, Irmgard: Discontinuous Automatic Control of Missiles. Tech. Rep. No. 14, (Contract N6-ONR-251 Task Order 2(NR-041-943) Office Air Res. and Office Naval Res.), Stanford Univ.  
Pt. 1, chs. 1-4, June 1950.  
Pt. 1, ch. 5, Aug. 1950.  
Pt. 2, chs. 6-8, Apr. 1951.  
Pt. 3, chs. 9-10, Dec. 1951.
7. Draper, C. S., and Schliestett, G. V.: General Principles of Instrument Analysis. Instruments, vol. 12, no. 5, May 1939, pp. 137-142.
8. Mueller, R. K.: The Graphical Solution of Stability Problems. Jour. Aero. Sci., vol. 4, no. 8, June 1937, pp. 324-331.

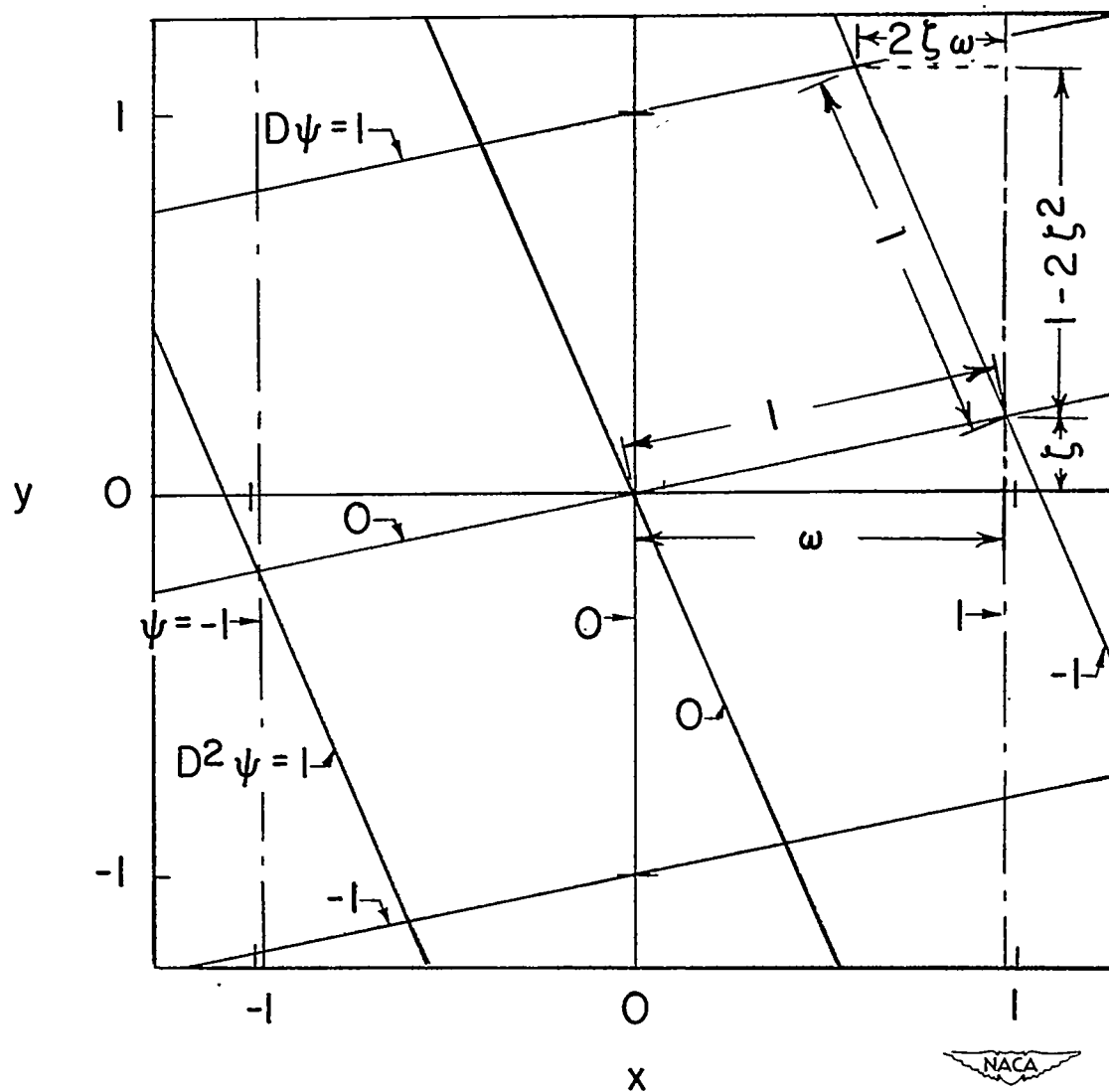
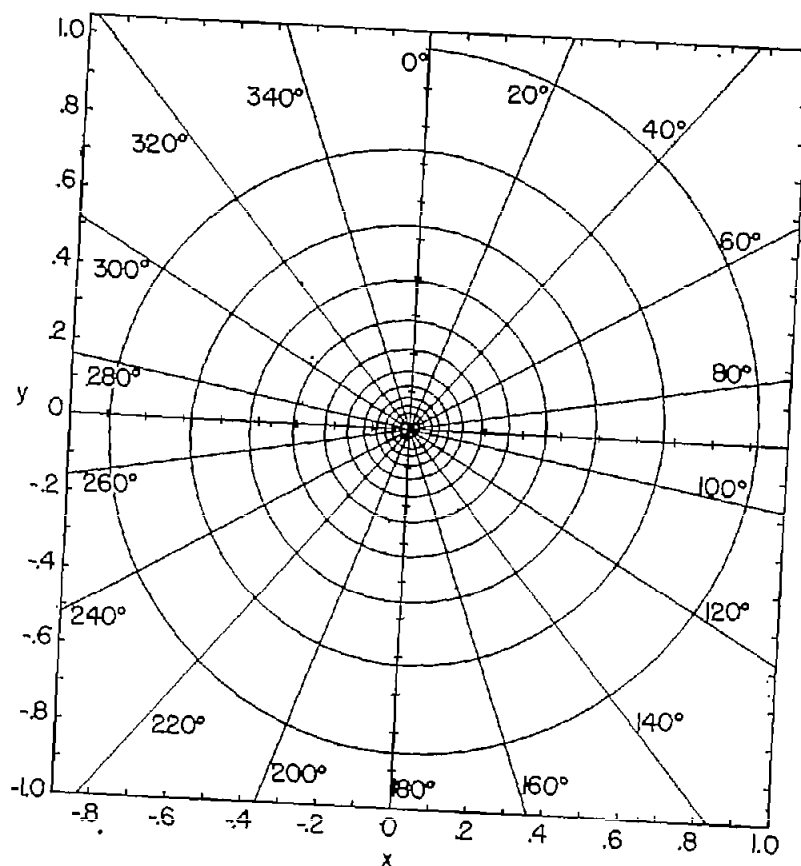
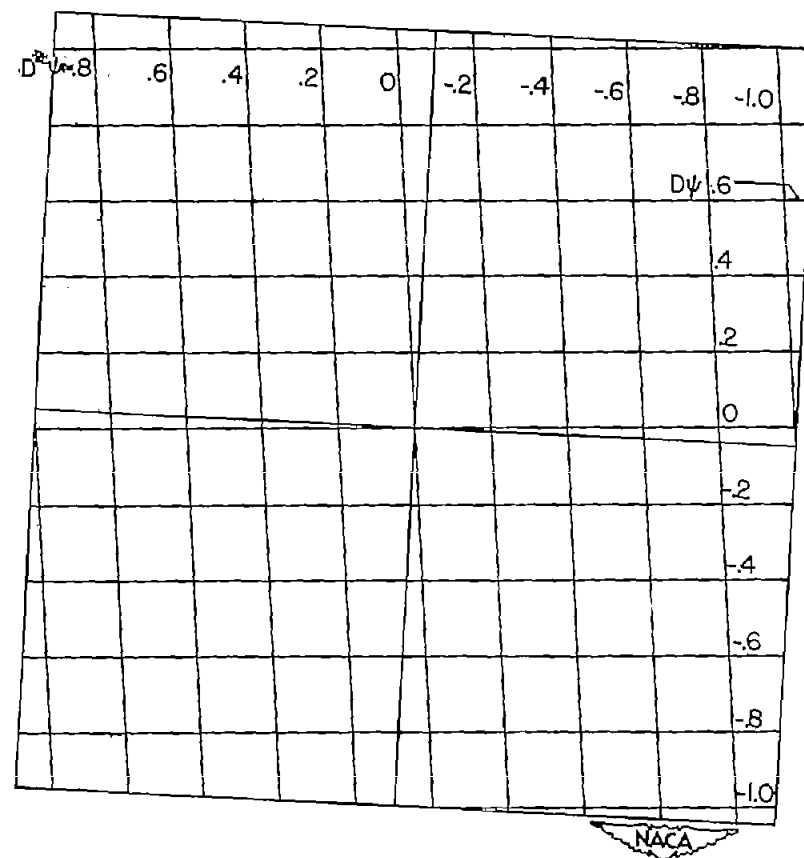


Figure 1.- Geometric relationship between the grid lines for reading  $D^2\psi$ ,  $D\psi$ , and  $\psi$ .

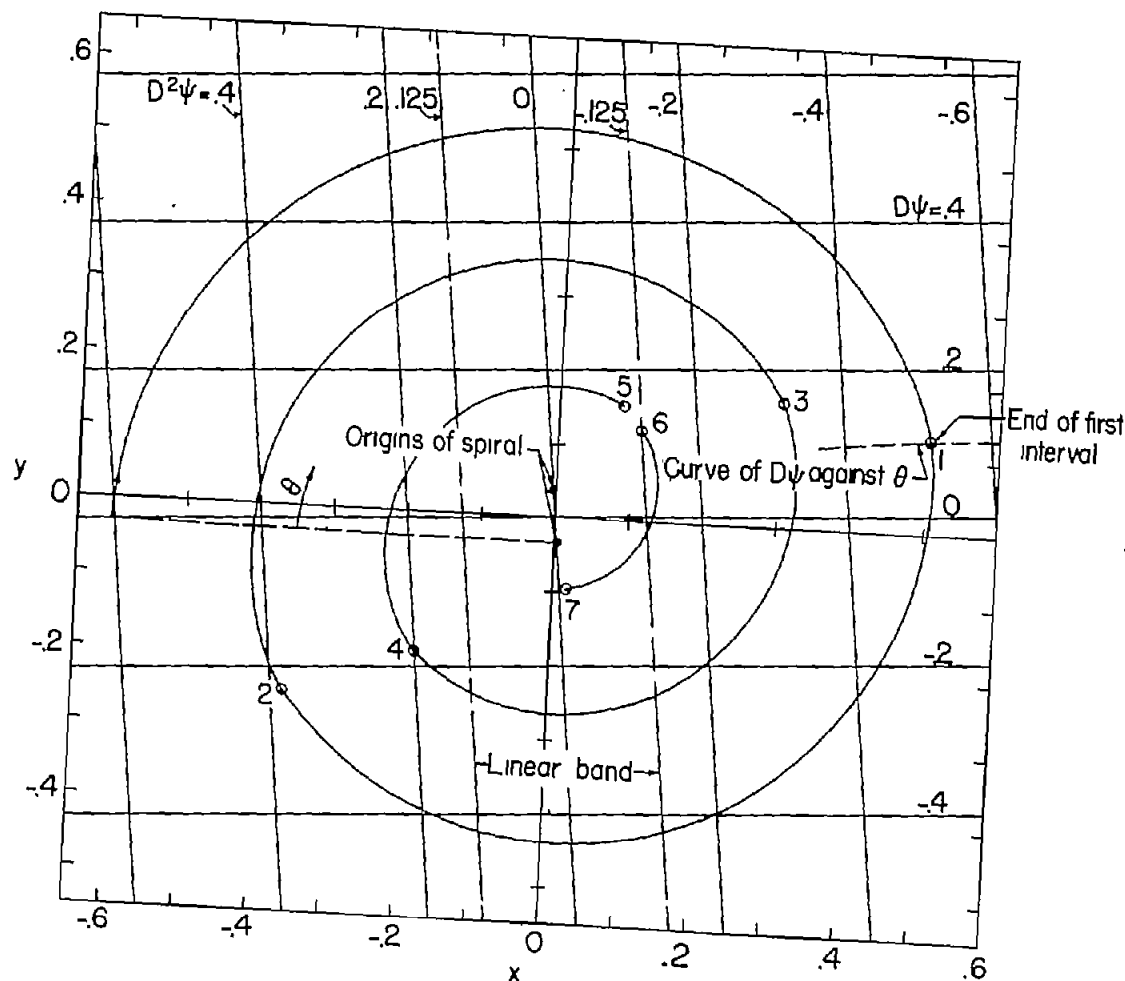


(a) Spiral for  $\zeta = 0.05$ .

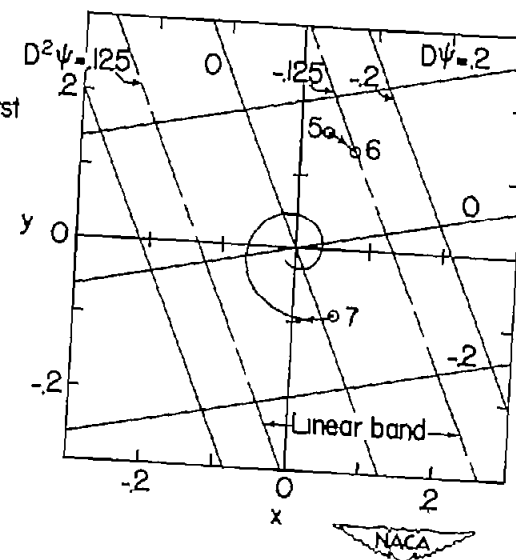


(b) Grids for reading  $D^2\psi$  and  $D\psi$ .

Figure 2.- Typical spiral and associated grids for reading  $D^2\psi$  and  $D\psi$ .



(a) Trajectories for nonlinear range of operation ( $\xi = 0.05$ ).



(b) Trajectories for linear range of operation ( $\xi_c = 0.2$ ).

Figure 3.- Graphical construction for example I.

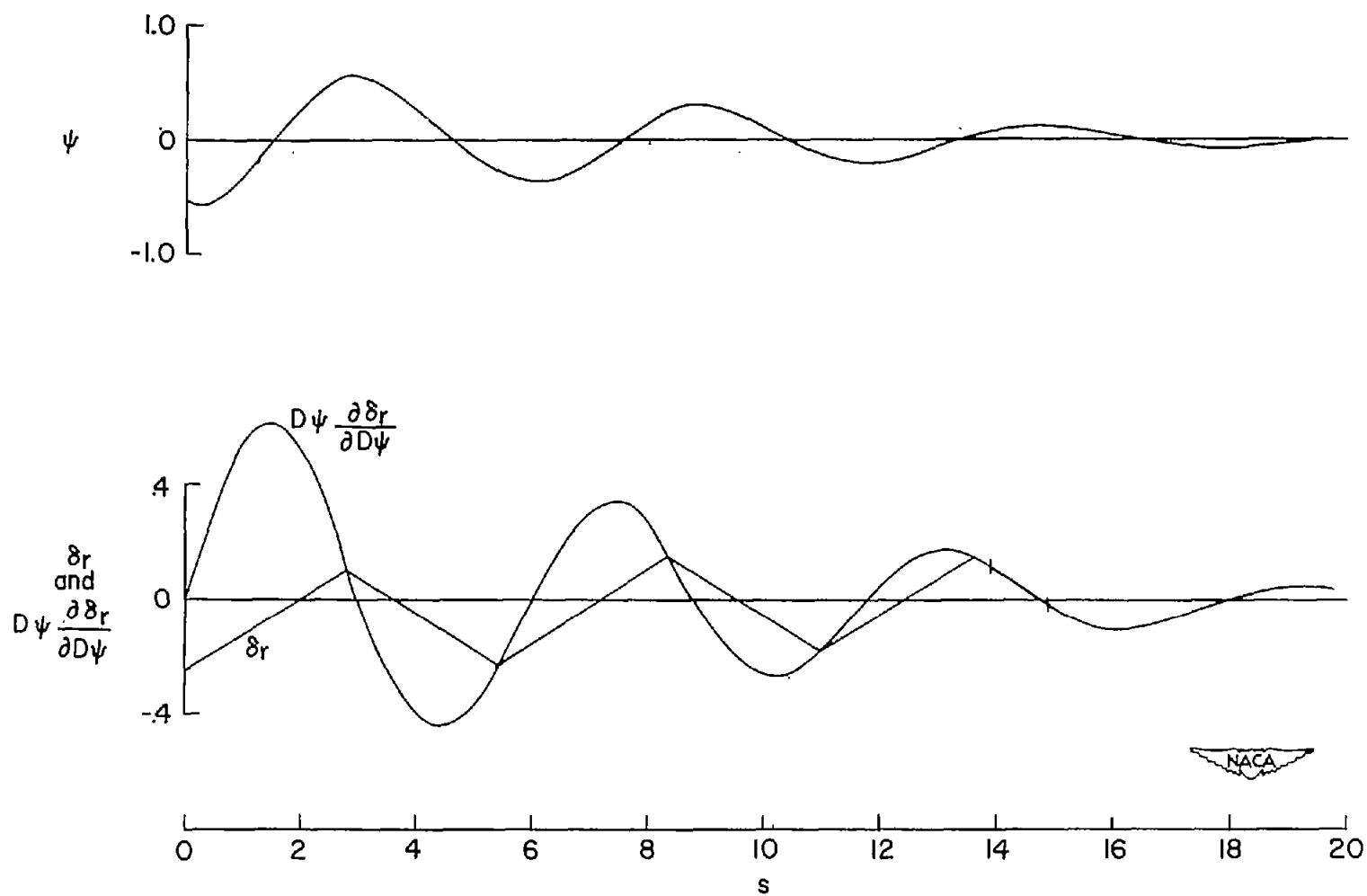
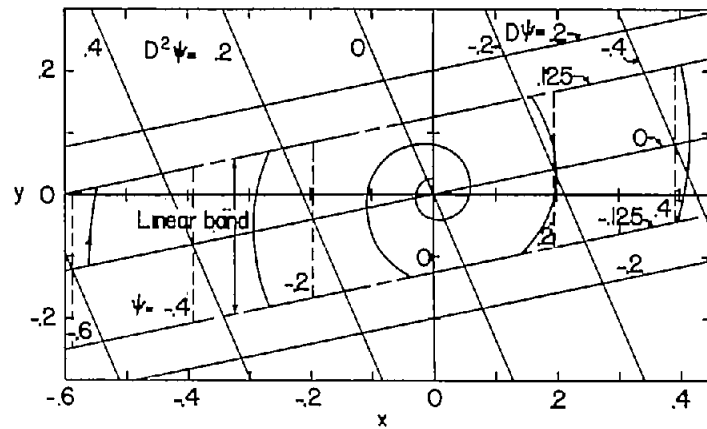
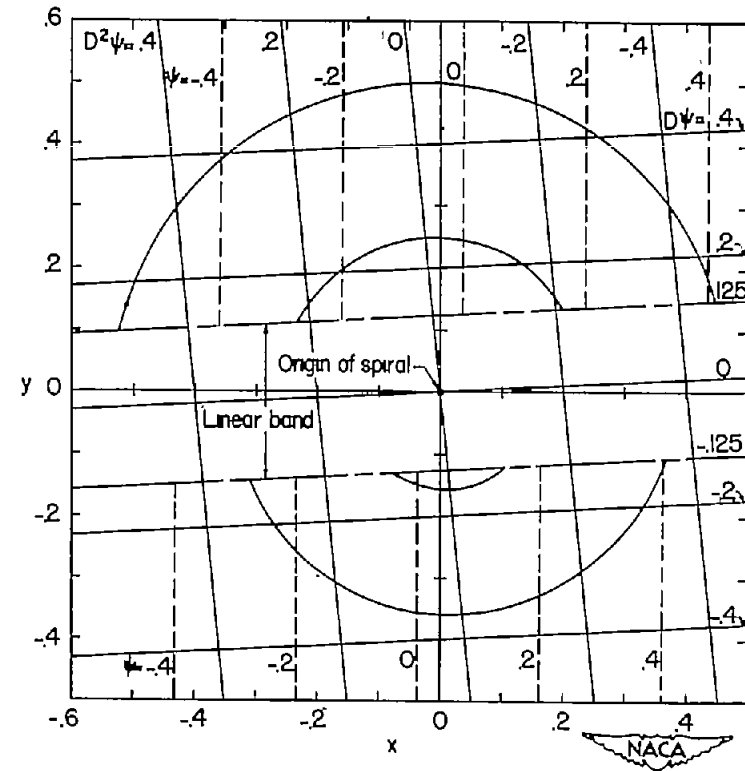


Figure 4.- Time histories of the angle of yaw  $\psi$ , the control function  $D\psi \frac{\partial \delta_r}{\partial D\psi}$ , and the rudder angle  $\delta_r$  for example I.





(a) Trajectories for linear range of operation ( $\xi_c = 0.2$ ).



(b) Trajectories for nonlinear range of operation ( $\xi = 0.05$ ).

Figure 5.- Graphical construction for example II.

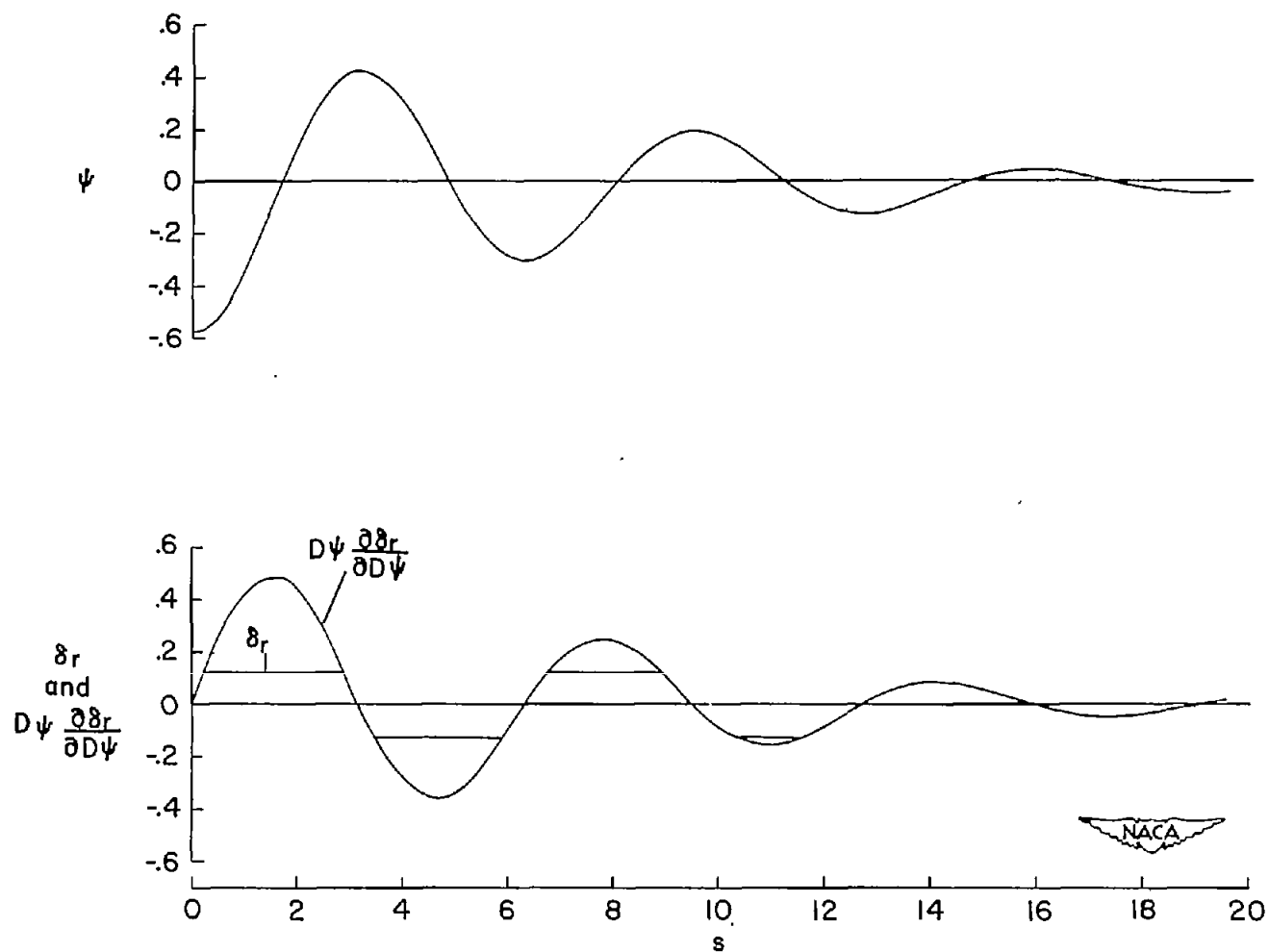
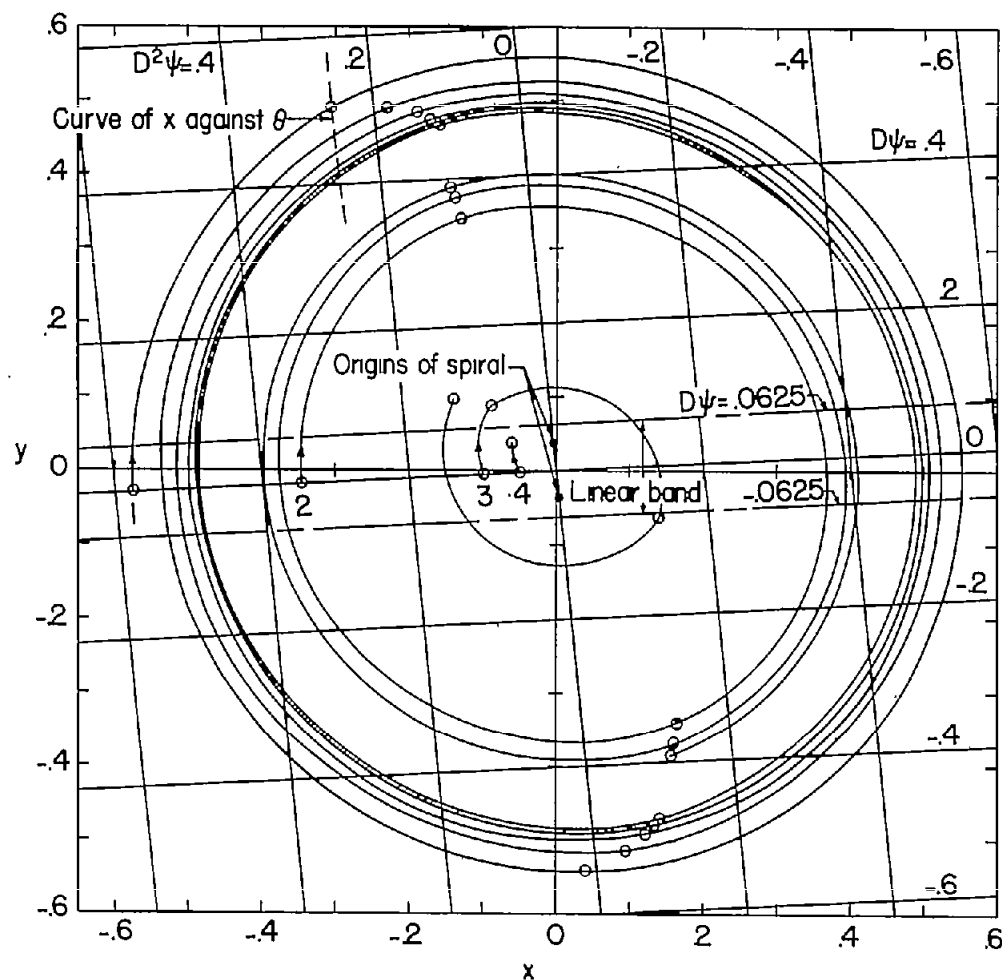
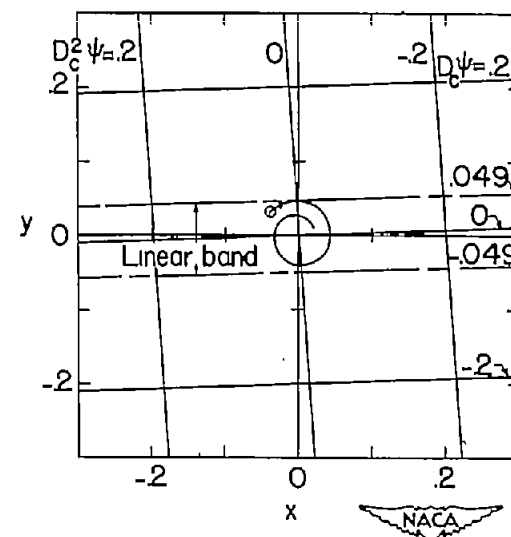


Figure 6.- Time histories of the angle of yaw  $\psi$ , the control function  $D\psi \frac{\partial \delta_r}{\partial D\psi}$ , and the rudder angle  $\delta_r$  for example II.



(a) Trajectories for nonlinear range of operation ( $\zeta = 0.05$ ).



(b) Trajectory for linear range of operation ( $\zeta_c = 0.0395$ ).

Figure 7.- Graphical construction for example III.

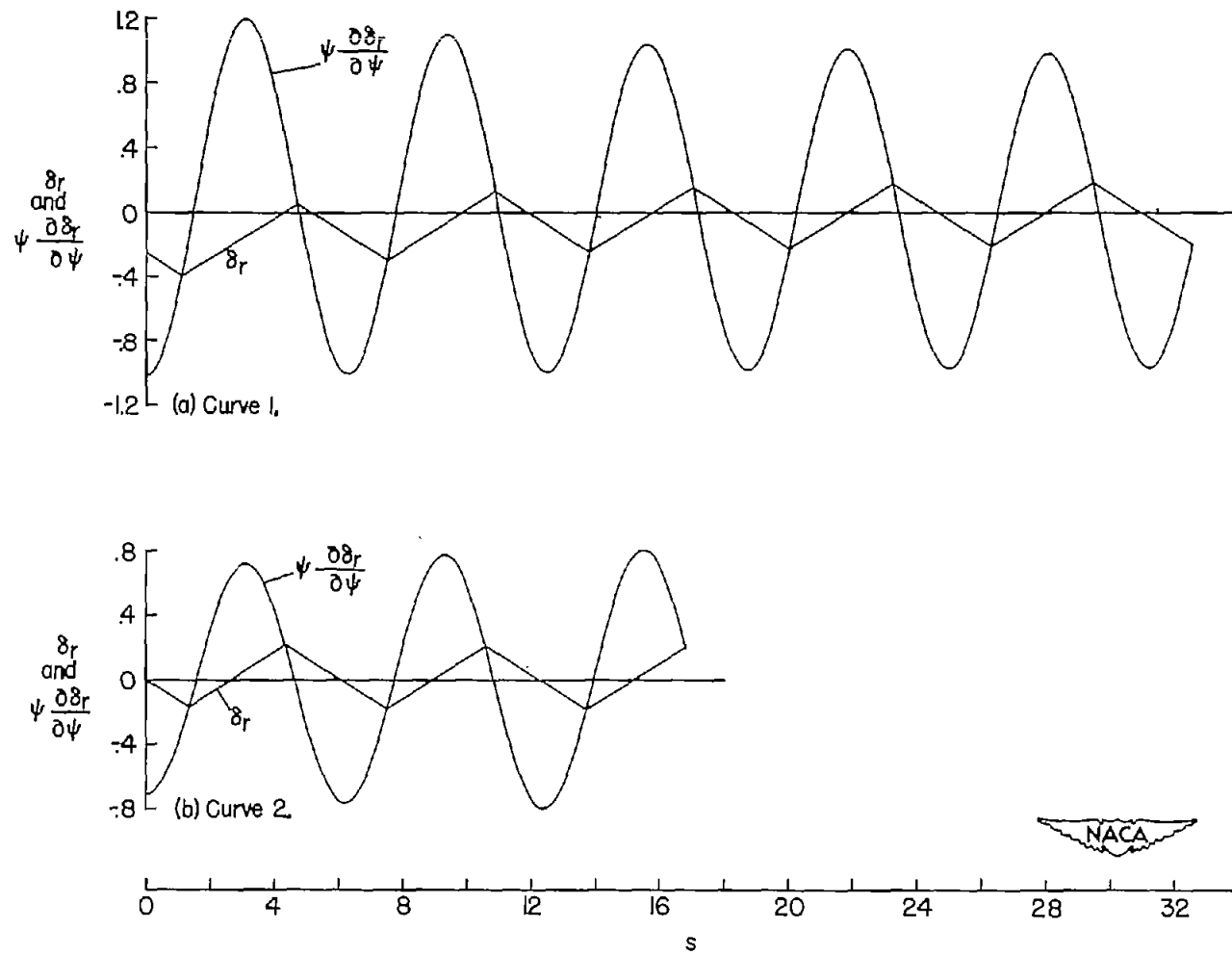


Figure 8.- Time histories of the control function  $\psi \frac{\partial \delta_r}{\partial \psi}$  and the rudder angle  $\delta_r$  for example III.

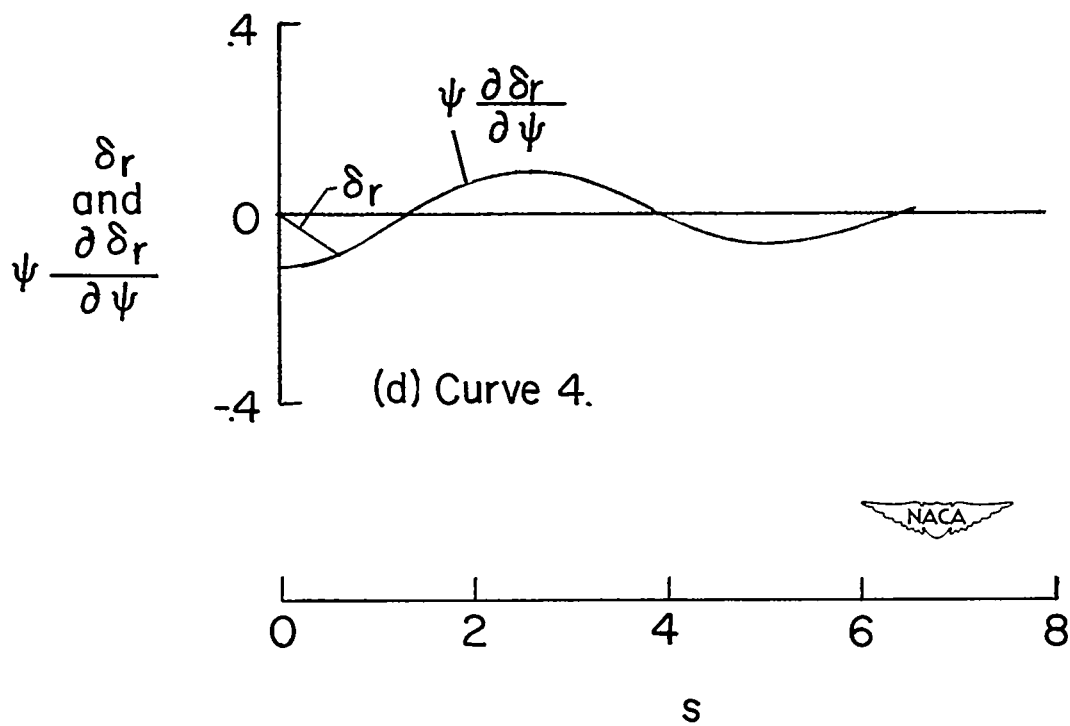
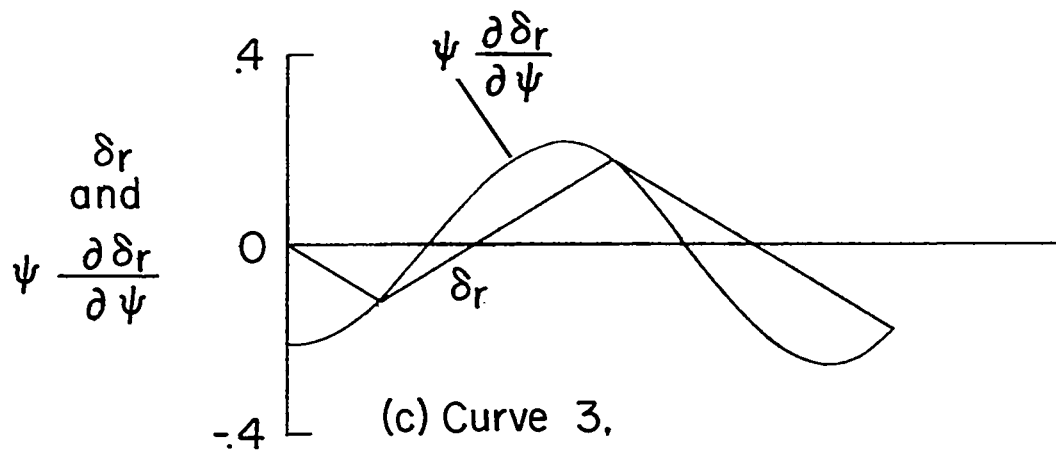
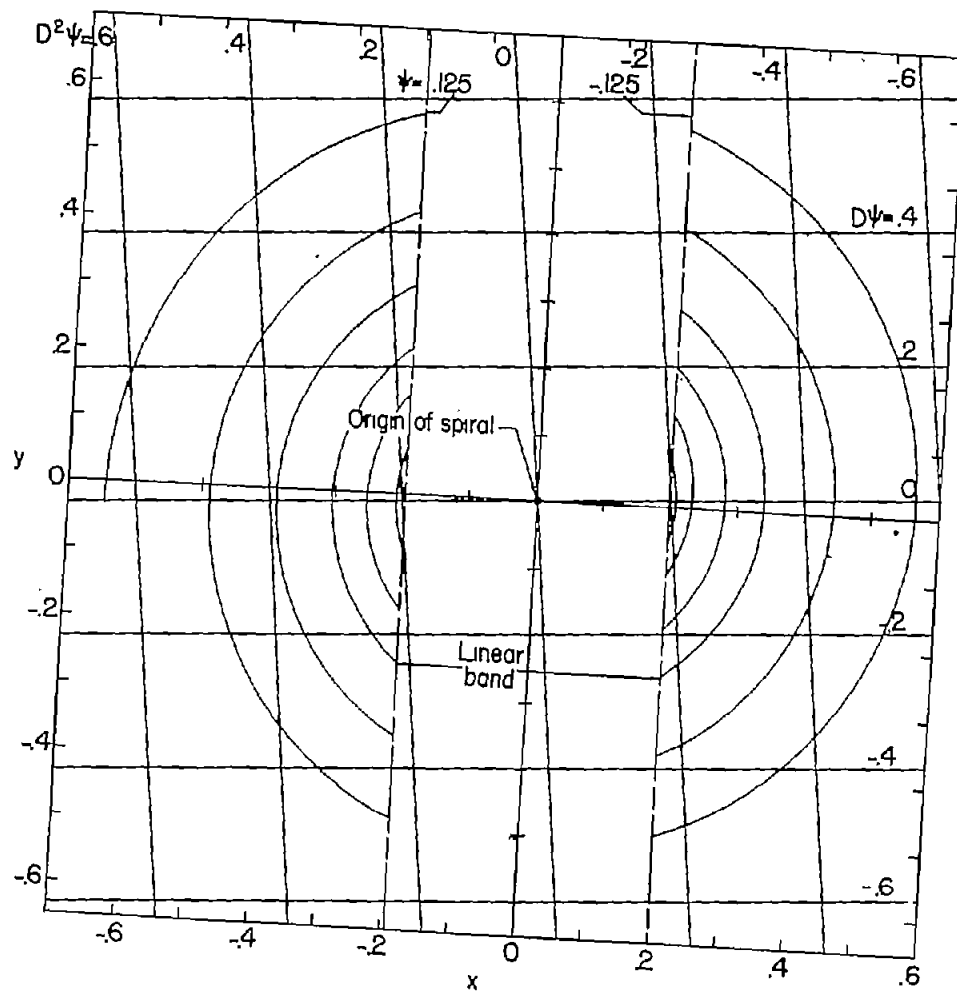
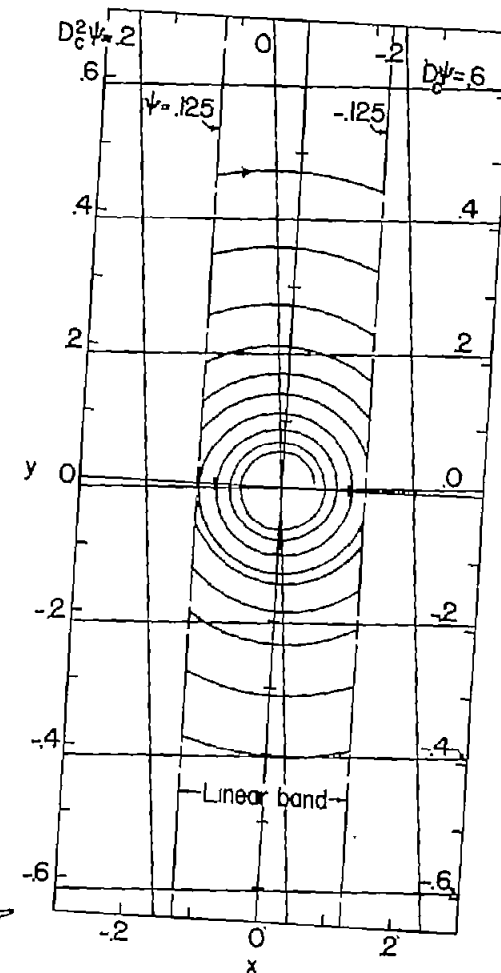


Figure 8.- Concluded.



(a) Trajectories for nonlinear range of operation ( $\zeta = 0.05$ ).



(b) Trajectories for linear range of operation ( $\zeta_c = 0.0395$ ).

Figure 9.- Graphical construction for example IV.

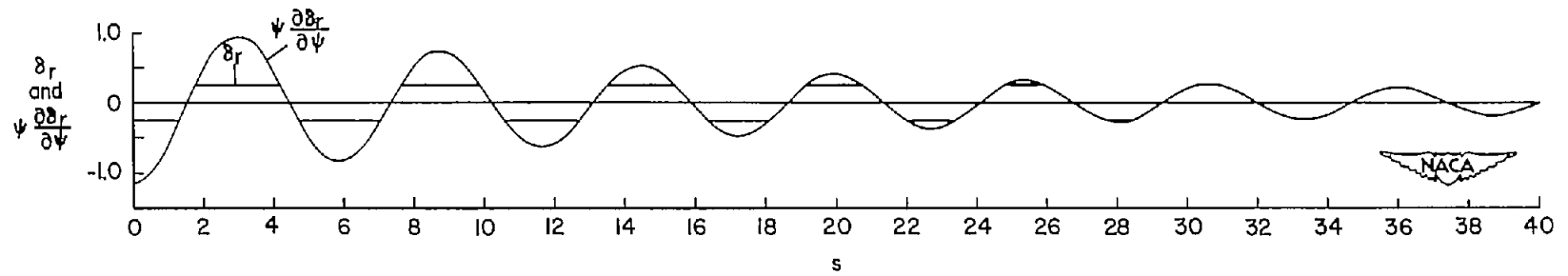
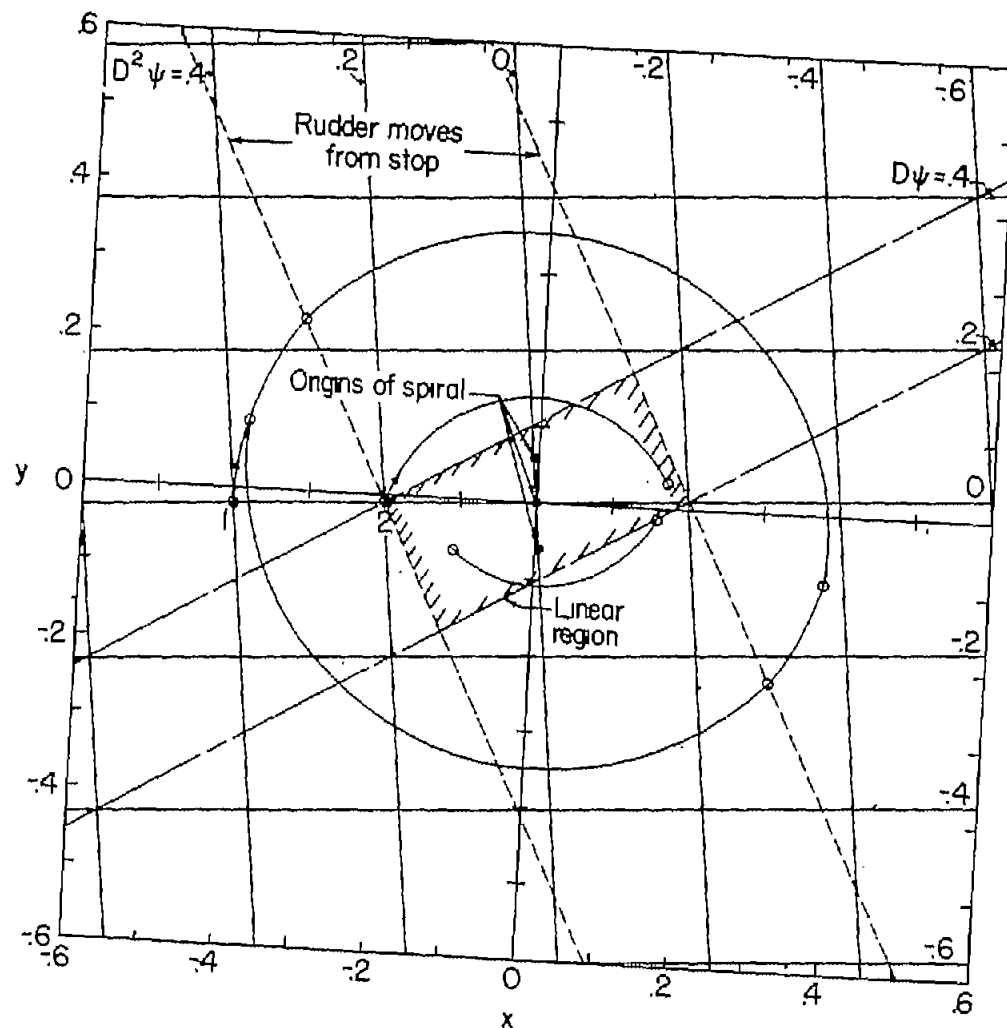
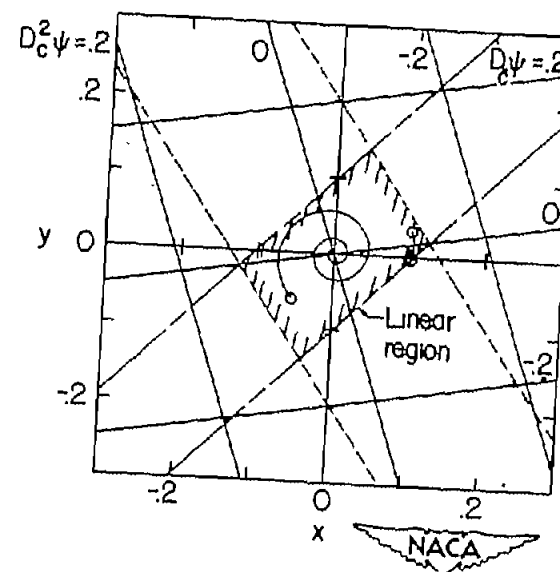


Figure 10.- Time histories of the control function  $\psi \frac{\partial \delta_r}{\partial \psi}$  and the rudder angle  $\delta_r$  for example IV.



(a) Trajectories for nonlinear range of operation ( $\xi = 0.05$ ).



(b) Trajectories for linear range of operation ( $\xi_c = 0.158$ ).

Figure 11.- Graphical construction for example V.



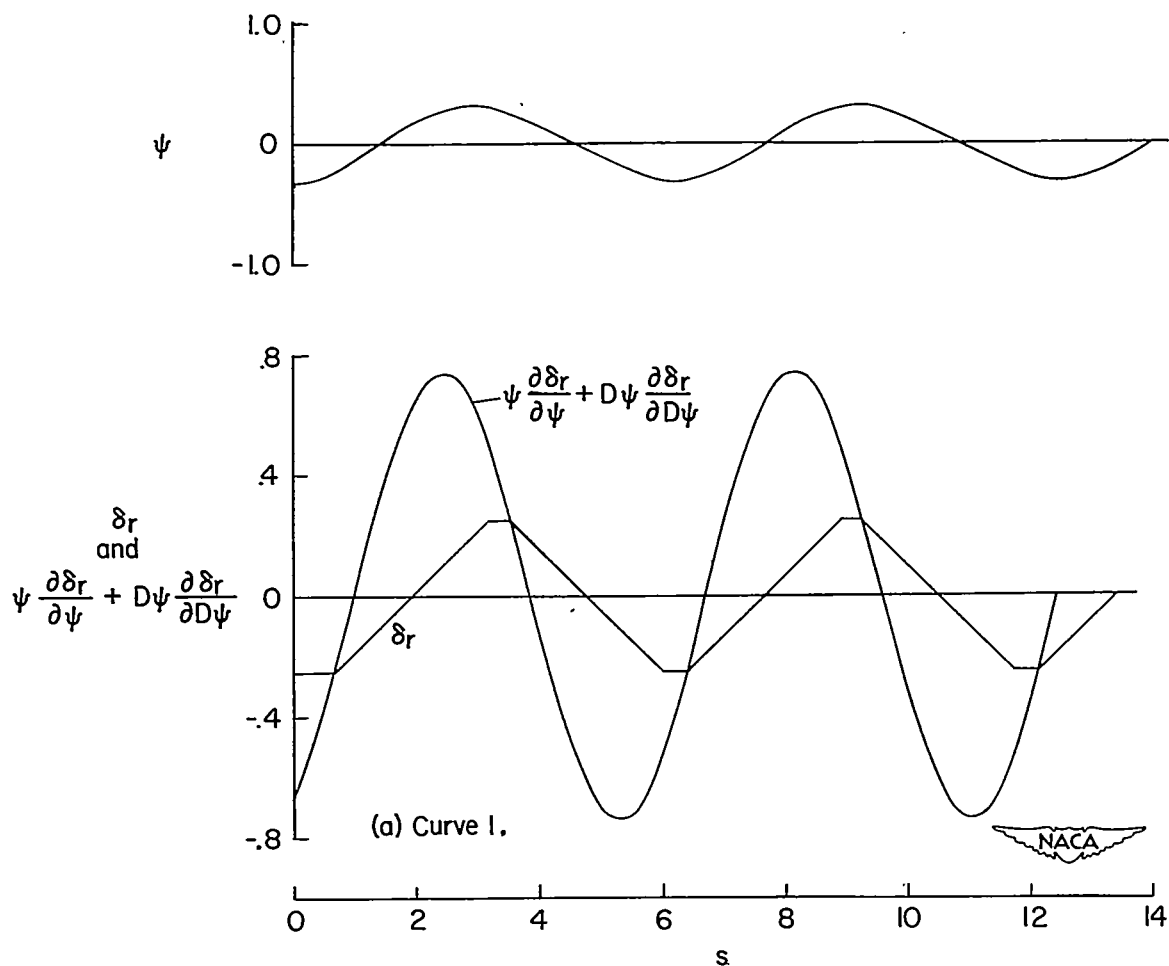


Figure 12.- Time histories of the angle of yaw  $\psi$ , the control function  $\psi \frac{\partial \delta_r}{\partial \psi} + D\psi \frac{\partial \delta_r}{\partial D\psi}$ , and the rudder angle  $\delta_r$  for example V.

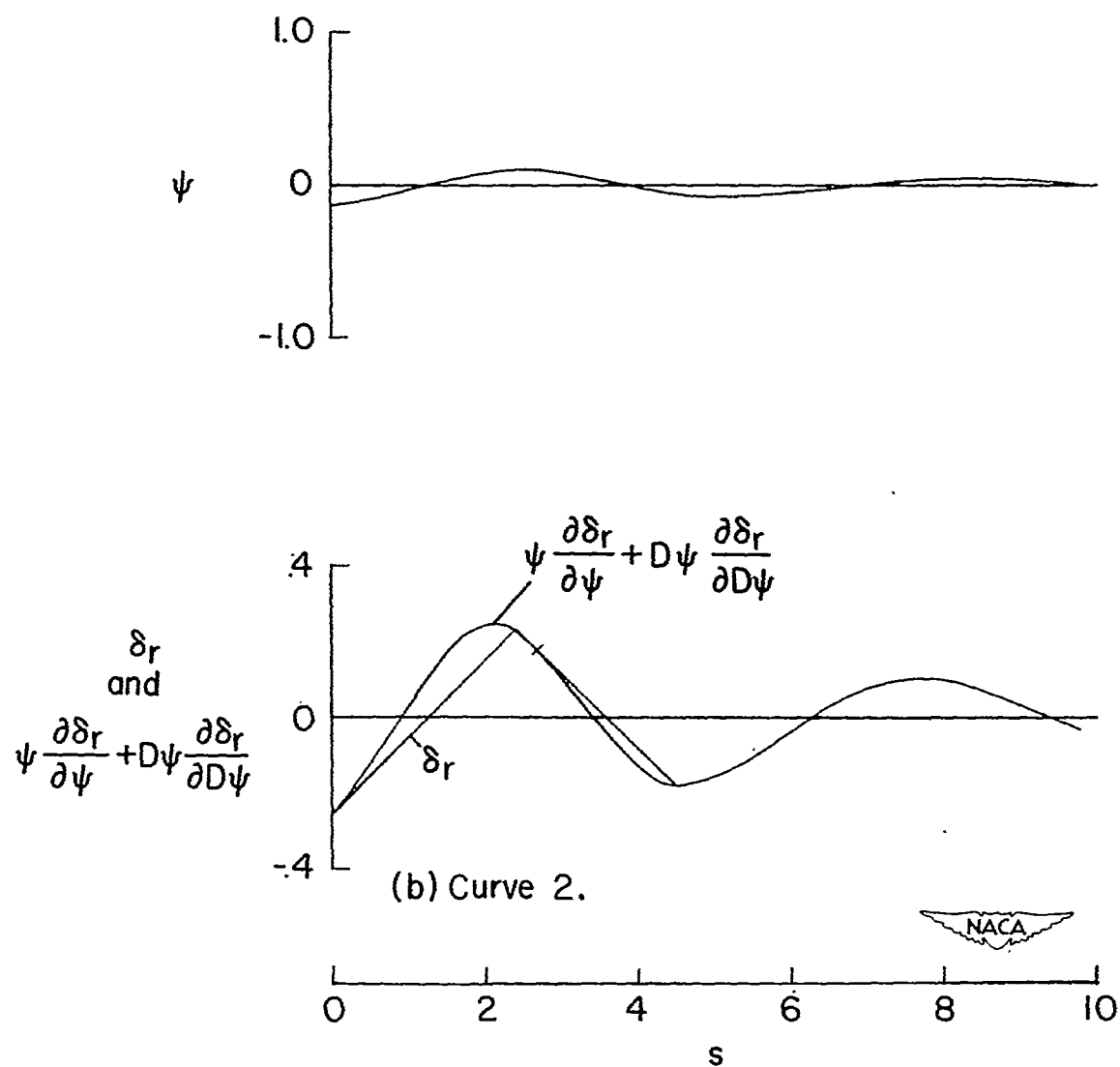


Figure 12.- Concluded.